Vanishing gap in LiF for electronic excitations by slow antiprotons

Beate Solleder,[1] Ludger Wirtz,[2] and Joachim Burgdörfer[1]
[1]*Institute for Theoretical Physics, Vienna University of Technology, 1040 Vienna, Austria, EU*
[2]*Institute for Electronics, Microelectronics, and Nanotechnology (CNRS, UMR 8520), Department ISEN, 59652 Villeneuve d'Ascq Cedex, France, EU*
(Received 31 October 2008; published 10 March 2009)

We study the influence of antiprotons and protons traveling through LiF on the band structure of the insulator using the embedded-cluster method. The crystal is represented by $F_m^- Li_n^+$ clusters with up to 19 fluorine ions embedded in a lattice of point charges representing the remainder of the crystal. The minimum excitation energy of LiF perturbed by the (anti)proton impurity is calculated employing the multiconfiguration self-consistent field method. The repulsive potential of the antiproton causes a dramatic local perturbation of the LiF band structure. We find a strong suppression of the excitation energy by more than an order of magnitude compared to that of the unperturbed crystal. The present results provide a simple explanation of recent stopping-power experiments for antiprotons in LiF which, surprisingly, found a "metal-like" behavior of the wide-band-gap insulator LiF. Our results also agree with recent experimental data indicating a deviation from metallic behavior of the stopping power of proton projectiles.

DOI: 10.1103/PhysRevB.79.125107 PACS number(s): 34.50.Bw, 34.50.Fa, 36.10.−k, 78.70.−g

I. INTRODUCTION

The specific energy loss $(-dE/dx)$ or stopping power of slow light ions continues to be of considerable interest .[1–5] Apart from fundamental aspects, the detailed knowledge of the energy deposition in the target along the projectile path is important for technical and medical applications such as ion-beam analysis or radiotherapy. Of particular interest is the comparative analysis of charge conjugated projectiles of equal mass, protons (p), and antiprotons $(\bar{p})$. At high projectile energies, where perturbation theory applies, differences due to corrections beyond the first-order term, the so-called Barkas corrections, have been studied in detail.[6–9] At low energies where perturbation theory fails and a fully self-consistent treatment of the electronic structure of the projectile-target complex is required, the analysis of stopping-power differences is far from well understood. Antiprotons play a special role as they represent the simplest realization of a Coulomb point charge. They are not subject to exchange interaction like electrons and, unlike protons, the repulsive Coulomb interaction with the target electrons precludes charge transfer and thus blocks a three-body reaction channel which can be both exothermal (superelastic) and endothermal (inelastic).

Recent measurements using protons and antiprotons found, surprisingly, that the stopping power dE/dx is proportional to the projectile velocity v_p at low kinetic energies for large-band-gap insulators. Such characteristics typically reflect metallic behavior and can be derived from simple electron-gas models. The key assumption is that electronic excitations occur for an arbitrarily small amount of energy transfer. Conduction electrons near the Fermi edge can be excited to low-lying states of the conduction band. Such a "gapless" excitation spectrum is in sharp contrast to wide-band-gap insulators where the energy gap between valence and conduction bands or excitonic states can easily be of the order of ~10 eV. Consequently, strong deviations from metallic behavior are to be expected for low projectile velocities. A simple estimate for the threshold energy E_p^c (or projectile velocity v_p^c) below which the excitation gap E_g becomes important can be derived from the (maximum) energy transfer during a classical binary head-on collision of an electron with an (anti)proton. Deviation from metallic behavior is expected for projectile kinetic energies E_p^c below[10]

$$E_p^c < \frac{M}{2m}\left[E_e - \sqrt{E_e(E_e+E_g)} + \frac{E_g}{2}\right], \tag{1}$$

where M and m are the projectile and electron mass, respectively, and E_e is the electron kinetic energy. For the large-band-gap insulator LiF with $E_g \simeq 14$ eV one can estimate the onset of a deviation from metallic behavior near $E_p^c \sim 3.6–5.3$ keV where we use the free-electron mass for m_e. The lower limit of this estimate for E_p^c corresponds to the collision with a "hot" electron (with velocity $v_e=0.3$ a.u.) while the upper limit corresponds to a collision with a "cold" electron ($v_e=0.1$ a.u.) in the valence band of LiF. Taking into account excitonic states in the band gap[11] would reduce E_g only slightly to about $E_g \simeq 12.7$ eV (Ref. 12) without a significant lowering of E_p^c within the error interval of this estimate.

For protons in LiF a deviation from the velocity proportionality of the stopping power was found recently by Draxler *et al.*[1] for proton kinetic energies below 3.8 keV. Stopping-power experiments using antiproton projectiles have been reported for energies down to 4 keV where the measured data are still consistent with metallic behavior of LiF.[2] The appearance of a possible deviation from metallic behavior of LiF in antiproton stopping-power experiments at very low kinetic energies is still an open question.

First calculations of the stopping power within the framework of time-dependent density-functional theory (TDDFT) have recently become available.[13] The energy gain of a periodic LiF supercell was measured as the projectile (proton or antiproton) passes through with constant velocity. In the present paper we provide complementary information.

Within a static calculation, we evaluate the electronic energy levels that contribute to the stopping power and determine the excitation threshold. Through the use of quantum-chemistry methods, electron correlations can be approximately accounted for. This allows us to gain insight into the microscopic mechanisms which are responsible for energy loss at very low projectile velocities.

The starting point of our analysis is the observation that the band gap of the unperturbed crystal (possibly reduced by excitonic excitations) may not be the appropriate quantity to start with in the presence of the strong perturbation by slow antiprotons.[14–16] In analogy to the Fano-Lichten effect[17] for positively charged ions and the Fermi-Teller effect[18] for antiprotons in the gas phase, energy levels of the crystal are shifted due to the perturbation by (anti)protons. Consequently, the energy gaps between the bands may be altered. More precisely, the presence of the antiproton can lead to localized states. Transition energies between these states may strongly deviate from those of the unperturbed band gap. Such a change in the effective gap would, in turn, shift the onset of a deviation from $dE/dx \propto v_p$.

In the present work we study the influence of antiprotons on the band structure of LiF by *ab initio* calculations. For comparison, we also perform calculations using proton projectiles where we focus on the dominant energy-loss channel corresponding to the conversion of the proton to neutral hydrogen.[15] Using an embedded-cluster approach we determine the electronic excitation gap in LiF when the solid is quasistatically perturbed by the external charge. We will show that the change in the excitation energy due to the perturbation by an antiproton is dramatic. The excitation threshold is reduced by more than an order of magnitude. "Metallic" behavior of the stopping power can therefore be expected down to much lower energies than previously assumed.

II. THEORETICAL METHOD

The theoretical treatment of the interaction of a slowly moving external charge with a crystalline solid is a challenging task as elements from solid-state physics as well as from atomic physics enter its description. Generically, methods used in solid-state band-structure calculations exploit the periodicity of the lattice. For lower-dimensional structures, e.g., surfaces, periodicity is enforced by supercell methods. In the present case the translational symmetry is strongly broken in all directions by a pointlike (zero-dimensional) perturbation. We therefore simulate an LiF crystal by $F_m^- Li_n^+$ clusters with $m \leq 19$ and $n \leq 40$ (Fig. 1). The calculations are performed for clusters of increasing size in order to verify convergence as a function of cluster size. For the construction of such a cluster it is important that every F^- is surrounded by Li^+ ions to avoid artificial distortion of the electron density.[19] The active ions are embedded in a lattice of point charges to ensure the proper inclusion of the Madelung potential.[20] This embedded-cluster method (ECM) has been successfully used in different studies on ionic crystals (e.g., Refs. 20 and 21, and references therein).

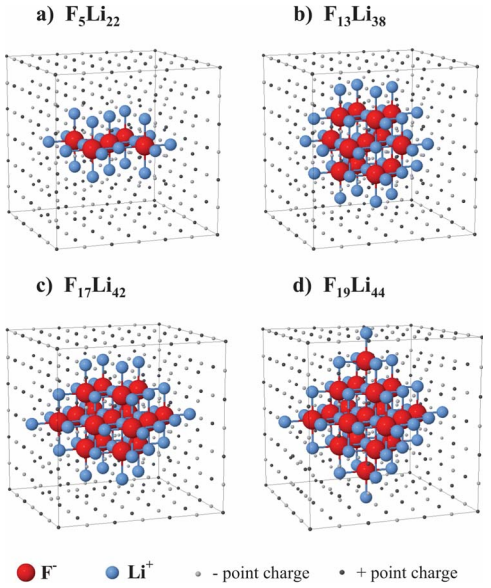

FIG. 1. (Color online) Representation of the LiF crystal by embedded clusters. Clusters studied in the present work are depicted.

We solve the stationary Schrödinger equation $\hat{H}\Psi = E\Psi$ in the Born-Oppenheimer (BO) approximation for the N-electron system consisting of the cluster plus the external antiproton or proton. The BO approximation is justified as starting point for low-energy transmission processes. The threshold for inelastic processes is governed in the low-energy limit by the leading-order nonadiabatic correction (of the Landau-Zener[22] or Rosen-Zener type[23]) relative to the adiabatic, i.e., Born-Oppenheimer potential hypersurface. The threshold can therefore be, to a good degree of approximation, determined from the BO surfaces without performing a full dynamical calculation. Clearly, the latter is required for a quantitative determination of the stopping cross section.

We study the dependence of the perturbation of the LiF band structure on the position of the projectile within the crystal using *ab initio* calculations on two different levels of accuracy. First, self-consistent field (SCF) or Hartree-Fock (HF) calculations are performed to determine the band gap of the perturbed crystal. The SCF ansatz for the N-electron solution $\Psi(\vec{\mathbf{r}}_1, \ldots, \vec{\mathbf{r}}_N)$, with $\vec{\mathbf{r}}_i$ including all spatial and spin coordinates, is given by a Slater determinant of the occupied molecular orbitals (MOs) of the system. Every molecular orbital ϕ_j is expanded in a finite Gaussian basis set $\phi_j = \Sigma_i \beta_{ij} \chi_i$. Due to the approximation of the solid by a finite cluster the electronic energy bands of the crystal are represented by discrete molecular levels. The density of the levels increases with cluster size. In an LiF cluster the valence band is approximated by the MOs predominantly built up by F $2p$-like basis functions and the conduction band by MOs predominantly built up by Li $2s$- and F $3s$-like basis functions. The band gap of LiF perturbed by external protons and antiprotons is given by the energy difference between the highest occupied molecular orbital (HOMO) and lowest unoccupied molecular orbital (LUMO) obtained from the SCF calculations.

As the SCF method is a mean-field theory, it allows us only to estimate changes in the band gap by the perturbing

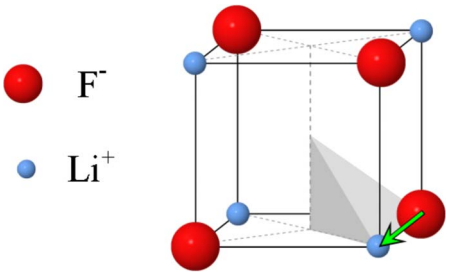

FIG. 2. (Color online) Unit cell of LiF. Gray shading indicates the irreducible volume within which the projectile positions were distributed. Results presented in Secs. III and IV correspond to projectile positions along the connecting line between F^- and Li^+ indicated by the (green) arrow.

(anti)proton on an independent-particle level. In order to go beyond the mean-field response and to include correlation effects, we also perform multiconfiguration self-consistent field (MCSCF) calculations.[24] On the MCSCF level, the N-electron solution Ψ is expressed as a linear combination of different configuration state functions (CSFs) Φ_l, $\Psi = \Sigma_l \alpha_l \Phi_l$. Every Φ_l is an N-electron Slater determinant representing a particular electron configuration with the N electrons distributed over the molecular orbitals of the system. The weighting of the different configurations is given by the coefficients α_l. Within the MCSCF calculation the coefficients α_l and β_{ij} are optimized simultaneously. Through the superposition of several configuration state functions an important part of electron correlation is taken into account as opposed to HF calculations where only one Slater determinant is considered. To determine the electronic excitation threshold of the system under study we have to calculate the ground state and first excited state simultaneously. In this case a state-averaged MCSCF is performed; i.e., the CSF expansion coefficients α_l are optimized separately for each state while the MOs are determined such that the total energy averaged over both states is minimized. The quantum-chemistry code COLUMBUS (Ref. 25) is used for both sets of *ab initio* calculations, SCF and MCSCF.

In Secs. III and IV we will discuss the details of the SCF and MCSCF calculations and present the results obtained for the SCF band gap E_g and the MCSCF excitation energy E_{exc} as well as a comparison between these two methods.

III. SCF CALCULATIONS FOR THE PERTURBED BAND GAP

As a starting point, SCF calculations were performed on the $F_{19}Li_{44}$, $F_{17}Li_{42}$, and $F_{13}Li_{38}$ clusters for a discrete grid of projectile positions within the marked volume in Fig. 2 in the central unit cell of the clusters. The Hartree-Fock closed-shell approximation was employed where the electrons are distributed over the MOs in pairs of opposite spin. For the basis functions χ_i in the SCF calculations the Gaussian basis set of Schäfer *et al.*[26] was used $((7s,3p)/[3s2p]$ for F and $(6s)/[2s]$ for Li).[27] From calculations using larger basis sets, which is computationally feasible for smaller clusters, we estimate the accuracy level of the SCF calculations to about 1 eV. For the proton projectile we used a cc-pVDZ basis $((4s,1p)/[2s,1p])$ with additional diffuse functions $(1s,1p)$. Here, cc-p stands for "correlation consistent polarized" and VDZ for "valence double zeta"[28] indicating that the basis functions for the valence electrons consist of two basis functions of different angular momentum l per atomic orbital. This allows the electron density to adjust its spatial orientation to the particular molecular environment. Convergence tests showed that the calculations are well converged with respect to the proton basis set.

As the projectile breaks the symmetry of the cluster, the calculations were first performed at arbitrary projectile positions within the irreducible volume of the unit cell (see Fig. 2), i.e., in the absence of any point-group symmetry (or equivalently, in the C_1 symmetry). Inspection of the results revealed that the most relevant positions of the antiproton, where the band gap reaches a minimum, lie on the connecting line between a fluorine and an adjacent lithium. Therefore, the C_{2v} symmetry could be used in further calculations for the reduced set of positions of p and $\bar{p}$ along the connection line between the central F^- of the cluster (Fig. 1) and Li^+.

The density of states (DOS) obtained from SCF calculations on the $F_{13}Li_{38}$ cluster for different positions of the projectile along the connection line between the F^- and Li^+ is shown in Fig. 3. Here, the results for the band gap E_g for all projectile positions used have converged as a function of cluster size, with the difference between results for the $F_{19}Li_{44}$ and the $F_{13}Li_{38}$ clusters lying below 0.1 eV. The DOS was obtained by broadening the SCF energy levels by Gauss functions with a standard deviation of 0.01 a.u. For reference, the DOS for the unperturbed cluster is also shown in Fig. 3. As is well known,[29] the SCF calculation clearly overestimates the band gap defined as the total-energy difference between HOMO and LUMO. We obtain $E_g = 15.3$ eV compared to the literature value of about 14 eV.[30] While the absolute value of the unperturbed gap is clearly inadequately represented by the SCF, it is of interest to explore to what extent SCF can describe *changes* in the gap due to the perturbation by p or $\bar{p}$.

The presence of an antiproton influences the LiF band structure dramatically [Fig. 3(a)]. For all positions within the unit cell, E_g is significantly reduced relative to the neutral cluster due to the "promotion" of a few occupied states in the energy range of the neutral band gap [Fig. 3(b)]. For protons we also observe a change in the DOS, however, not nearly as dramatically as in the antiproton case.

Apart from the opposite charge, the main difference between the p and $\bar{p}$ projectiles is the ability of the proton to form molecular orbitals with the target ions and to capture electrons. For the stopping power this charge exchange constitutes an additional channel for energy loss (or gain) as opposed to $\bar{p}$ projectiles where the target electrons are perturbed by the repulsive field of the negative charge brought into the crystal. This also manifests itself in differences in the gap variation. While for a $\bar{p}$ projectile, both valence and conduction bands are shifted upward in energy, the energy shift of the bands is toward lower energies in case of a proton projectile. This is not surprising given the composition of the valence (F $2p$-like MOs) and conduction bands (MOs of

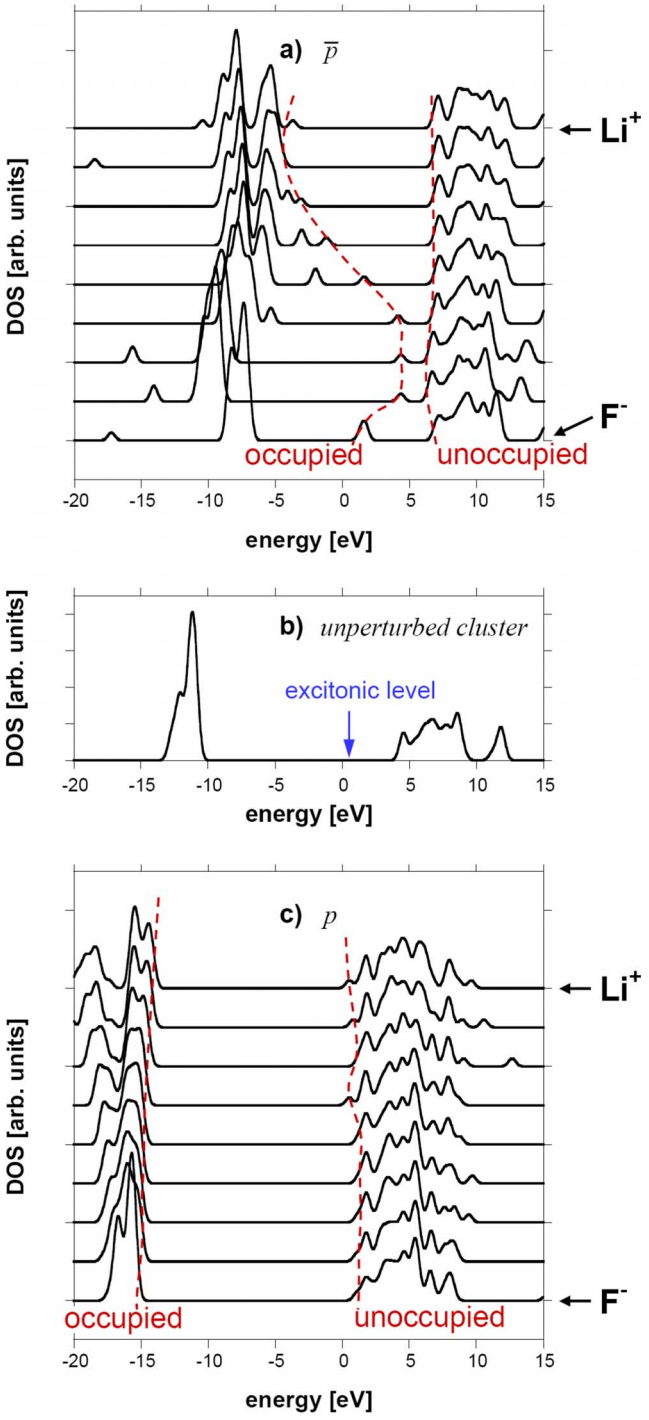

FIG. 3. (Color online) DOS for the $F_{13}Li_{38}$ cluster in SCF approximation for different positions of the projectile along the connecting line between F^- and Li^+. (a) Antiproton projectile, (b) unperturbed cluster, and (c) proton projectile. Dashed lines indicate the variation of the HOMO and LUMO with the position of the perturber. For the unperturbed cluster, the excitonic level is also shown (see text).

mixed Li 2*s* and F 3s-like character). As an antiproton approaches F^-, the negative charge of $\bar{p}$ effectively reduces the nuclear charge of F^- by 1 leading in the unified-atom limit to an isoelectronic configuration of O^{2-} which, in vacuum, is unbound (Fermi-Teller limit[18]). The HOMO of LiF is considerably shifted toward the vacuum level due to the presence of an antiproton. By contrast, a proton at the position of F^- would correspond in vacuum to replacing F^- with a neutral Ne atom with all electrons well bound. In this case, the valence band is shifted to lower energies [Fig. 3(c)].

In Fig. 3(b) the excitonic level is also marked at the energy $E_{\mathrm{HOMO}}+E_{\mathrm{exc}}$, where E_{HOMO} is the energy of the HOMO and E_{exc} is the energy needed to excite an exciton (see Sec. IV). Of course, excitons can also be excited in the LiF crystal when an (anti)proton is present and locally modifies the band structure. For clarity, the excitonic level is only shown for the unperturbed cluster in Fig. 3.

IV. MCSCF CALCULATIONS FOR THE EXCITATION GAP

While the SCF results already illustrate the influence of the (anti)protons on the LiF band structure, for a quantitative determination of the electronic excitation threshold, one has to calculate excitation energies which, in general, do not coincide with the band gap E_g. The excitation energy of an exciton is given by E_g reduced by the attractive electron-hole interaction. In a one-electron picture this corresponds to additional excitonic levels below the edge of the conduction band within the band gap [Fig. 3(b)]. In order to study the modified excitation energies, we perform state-averaged MCSCF calculations for different positions of the projectiles in the cluster calculating the ground state and the first excited state. From total-energy differences we obtain excitation energies E_{exc} which determine the threshold for electronic excitation in the presence of a proton or antiproton in LiF.

For computational reasons, the MCSCF is performed on smaller clusters (e.g., F_5Li_{22}). For the same reason, systematic convergence studies as a function of cluster size are currently not feasible. We therefore extrapolate the estimate for size error from our SCF studies: variations of cluster size of the unperturbed LiF crystal using the same basis set yield differences in E_g of about 0.6 eV between the value for F_5Li_{22} and $F_{13}Li_{38}$. Comparing the SCF results for different clusters with an antiproton present shows smaller variations, in particular at close distance of $\bar{p}$ to F^-, i.e., the region of the threshold. We therefore expect the systematic error due to cluster size effects to lie in the 0.1 eV range.

The (comparably) small number of active ions in the F_5Li_{22} cluster allows for the use of a larger basis set. For a convergence test of the basis set we have compared again SCF band gaps, now for the F_5Li_{22} cluster, using different basis sets of increasing size. The basis set is required to be both small enough to allow for computationally demanding calculations and large enough to be converged in the size of the basis set. For the F^- ions the optimal basis set is a cc-pVDZ $(9s,4p,1d)/[3s,2p,1d]$ basis with additional diffuse functions $(1s,1p)$, and for the Li^+ ions it is the $(7s/[3s])$ basis set of Schäfer *et al.*[26] For the proton projectile we take again the cc-pVDZ basis $((4s,1p)/[2s,1p])$ with diffuse functions $(1s,1p)$ already used for the SCF calculations. The variation of E_{exc} with basis set is about 0.1 eV.

In the MCSCF calculations we exploit the fact that the lowest values for E_{exc} are expected for positions of $\bar{p}$ along

the line connecting F^- with Li^+ (see Fig. 2). This allows us to utilize the C_{2v} symmetry group. In fact, the MCSCF calculations are performed in A_1 symmetry, the highest symmetry within the C_{2v} symmetry group, as the states of lowest energy are expected to have highest symmetry. Within the A_1 symmetry, a wave function remains unchanged under the symmetry operations, rotation by 180°, reflection at the x-z plane, and reflection at the y-z plane.

Within the so-called *complete active space self-consistent field* (CASSCF) method employed, all occupied and unoccupied MOs are divided into *active* and *inactive* orbitals. The inactive occupied orbitals are kept doubly occupied in all CSFs during the calculation; the unoccupied inactive orbitals, also called *virtual* orbitals, are kept empty. The remaining MOs form the active space among which the active electrons are distributed forming the different CSFs. The physics reasoning underlying this division into different types of orbitals is that the inner-shell (inactive) electrons are deeply bound to the nuclei. They occupy molecular orbitals very similar to the atomic orbitals of the free atoms. The overlap of the wavefunctions of inner-shell electrons with those of adjacent crystal atoms is very small. By contrast, weakly bound valence orbitals overlap with neighboring sites forming molecular orbitals and contribute to chemical bonding. The active space thus consists of the MOs of the valence electrons and low-lying unoccupied MOs.

In LiF the valence electron MOs are formed by the F $2p$ states and the lowest unoccupied MOs by the Li $2s$ and F $3s$ states. Therefore, for all calculations the F $1s$-, F $2s$-, and Li $1s$-like MOs are kept doubly occupied. The active space is divided into a restricted active space (RAS) from which only single excitations are allowed and a complete active space (CAS) where also double excitations are possible. All F $2p$-like MOs of A_1 symmetry are in the CAS while all F $2p$-like MOs of other symmetries are in the RAS. For the third part of the active space, the auxiliary orbitals (AUXs), i.e., MOs where electrons can be excited to, the lowest three A_1 MOs are used for calculations with a $\bar{p}$ projectile. This configuration space containing all MOs corresponding to the valence band of LiF is already well converged with respect to the size of the active space. For the p projectile calculations, only one MO could be included in the AUX for computational reasons. This leads to an uncertainty in the MCSCF results for proton projectiles which we estimate to be <1 eV from variations of the auxiliary space in calculations for smaller clusters.

For the unperturbed (neutral) cluster, the MCSCF calculations yield an excitation threshold of 10.8 eV corresponding to the excitation of an exciton (Fig. 4). The strong perturbation of the crystal band structure by an antiproton is even more pronounced than for the calculated SCF band gaps (Fig. 4). The extremely low excitation thresholds for distances z to F^- below 2 a.u. (found to be as small as ~ 0.44 eV) can be understood when we take a closer look at the dominant configurations contributing to the ground state and the first excited state. We find that in the state of lowest energy the F $2p$-like MOs are not all doubly occupied as one might expect for the ground state. Instead, one of these MOs (the highest in energy) is only singly occupied and so is the lowest Li $2s$-like orbital, i.e., there is already one hole in the valence band in the ground-state configuration. As the adjacent state higher in energy has a similar dominant configuration where just another Li $2s$-like MO is singly occupied, the two states of lowest energy are nearly degenerate. The excitation energy from the lowest to the next state is consequently very small. As in the ECM the conduction band is approximated by discrete levels, it is difficult to determine if the two (nearly) degenerate states would still be separated by a small gap in the limit of an infinitely extended crystal or if they both would already lie in the continuum of the conduction band. The latter case would imply even a vanishing excitation gap.

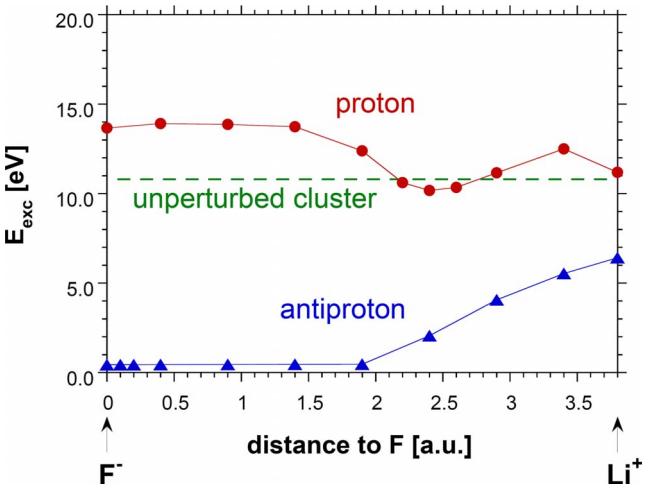

FIG. 4. (Color online) Dependence of the (MCSCF) excitation energy E_{exc} on the position of the antiproton and the proton along the connecting line between F^- and Li^+. The result for the unperturbed cluster is also shown. Lines are to guide the eyes.

Relating the perturbation caused by $\bar{p}$ at the F^- site to the unified-atom limit of an O^{2-} ion provides direct insight into the single MO occupations in the ground state. A free O^{2-} ion in vacuum is unstable such that the outermost electron would be unbound. Within the ionic crystal this outermost electron is promoted to the conduction band. The ground state consequently has a singly occupied HOMO. For a consistency check we have performed the MCSCF calculation also in an $O_1F_4Li_{22}$ cluster, i.e., we have replaced the central F in the F_5Li_{22} cluster with an oxygen atom and run the calculation with the same number of electrons as before. As expected, the results were nearly identical to the F_5Li_{22} cluster when the antiproton position is on top of the central F.

The promotion of the outermost electron to a higher orbital at close distances between $\bar{p}$ and F^- is similar to the Fermi-Teller effect. The latter refers to the promotion to the continuum of adiabatic potential curves in the $\bar{p}$- (one-electron) atom complex below a critical distance, the Fermi-Teller radius $r_{FT}=0.639/Z$ a.u. As our calculations are performed in the adiabatic approximation, dynamical effects leading to diabatic promotion are not accounted for. Our results for the threshold energy therefore represent a static limit providing an upper bound for E_{exc}. Dynamical effects such as transitions due to avoided crossings of the potential-energy surfaces may lead to an additional decrease in this threshold.

For $z>2$ a.u., the antiproton is near to the Li^+ site and the dominant configuration of the energetically lowest state is given again by the typical ground-state configuration with a doubly occupied HOMO of F $2p$ character. The excitation gap increases with increasing z reaching a maximum of $E_{exc}=6.42$ eV at the $\bar{p}$ position on top of Li^+. The increase in the excitation energy near Li^+ can be qualitatively understood in terms of the corresponding unified-atom limit in the gas phase of neutral helium featuring the largest excitation gap in the Periodic Table (19 eV). Clearly, embedding in the solid-state environment drastically reduces this value.

For protons as perturber (Fig. 4) the modification of the excitation gap is, by far, less pronounced. The variation as a function of position resembles the SCF results for the band gap. Of interest is the minimum at about 2.4 a.u. lying below the excitation energy of the neutral cluster also present in the SCF band-gap results. As this distance coincides with the typical spatial extension of an F $2p$ orbital, the dip may originate from the overlap and the formation of a quasimolecular orbital between F^- and H.

It is now instructive to compare the two methods employed, SCF and MCSCF. A multiconfiguration approach is clearly conceptually more suitable for the problem under study dealing simultaneously with the ground state as well as excited states. In principle, excited states can also be calculated by SCF. However, in the SCF the electronic configuration is fixed *a priori*, i.e., one has to know the distribution of the electrons among the MOs of the system before the minimum total energy of the system is determined by the SCF. By contrast, the MCSCF calculation employs the variation and superposition of different configurations. Apart from these technical details, the main difference between the two methods is correlation effects included only in MCSCF. In order to estimate the importance of correlation effects we have compared total energies of the ground and first excited states calculated with both methods where the dominant configurations obtained from MCSCF were used as configurations for the corresponding SCF. The contributions to energy differences ascribable to correlations are below 1 eV where we find smaller correlation contributions for configurations with an electron excited (or promoted) to the conduction band than for closed-shell ground states. The underlying reason is that open-shell HOMO configurations of excited states are more "one-electron like" than closed-shell configurations and can thus be better described by the independent-particle SCF theory.

An alternative strategy for a comparison between SCF and MCSCF is the determination of the perturber-induced changes in the excitation gap ΔE_g with respect to the unperturbed system (Fig. 5). While we consider $\Delta E_g=E_{exc}^{(p,\bar{p})}-E_{exc}$ for the MCSCF, we determine the changes in the band gap $\Delta E_g=E_g^{(p,\bar{p})}-E_g$ in case of the SCF (due to convergence problems in the calculation of excited states for $\bar{p}$ positions near F^-). The advantage of this analysis is that it allows for a direct comparison of the perturber-induced changes while removing perturber-independent contributions which, otherwise, make SCF and MCSCF results difficult to compare. For both antiprotons and protons (Fig. 5) the variations of the gap changes ΔE_g as a function of position resemble each other, in particular the lowering of the gap for $\bar{p}$ is most

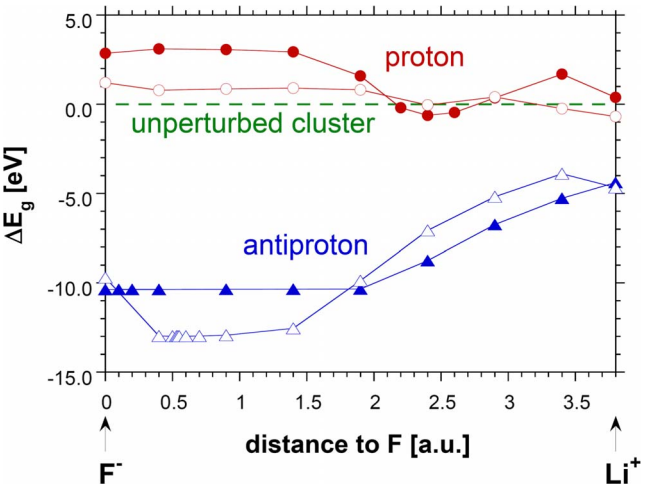

FIG. 5. (Color online) Comparison of the changes ΔE_g of the SCF band gap with those of the MCSCF excitation gap. Energy values are plotted relative to the excitation (band) gap of the unperturbed clusters. Open symbols: SCF and full symbols: MCSCF.

pronounced near F^- reflecting the Fermi-Teller effect in the solid. We note that for $z<2$ a.u., the SCF and MCSCF curves remain similar but they reflect different physical situations. In the SCF calculation, an excitation gap of 2.4 eV remains. This gap is due to the restriction to closed-shell configurations which artificially enforces the energetically highest electron to remain localized at the F ion. In the MCSCF calculation (which includes open-shell configurations) one electron has been promoted to the continuum of the conduction band through the repulsive potential of the antiproton. The slight lowering of the gap for protons located at a distance from F^- on the order of the typical bonding length is common to both MCSCF and SCF (Fig. 5).

Our results for the excitation threshold in the LiF cluster perturbed by antiprotons imply a drastic reduction in the antiproton kinetic energy below which a deviation from metallike behavior in the stopping power should occur. Estimating the onset of a deviation using Eq. (1) and the minimum excitation energy of 0.44 eV for E_g yields about $E_p^c \sim 10-70$ eV only, i.e., more than an order of magnitude smaller than previously expected and close to the threshold for excitation of an electron-hole pair or exciton. The lower limit of our estimate corresponds to $v_e=0.3$ a.u. of a hot electron and the upper limit to $v_e=0.1$ a.u. of a cold electron. Clearly, Eq. (1) based on a binary-encounter approximation can serve only as a rough estimate for the quantal transition near a Landau-Zener curve crossing. In addition, we note that our results for the excitation threshold provide an upper bound for E_{exc}. Accordingly, much lower antiproton energies than used in previous experiments would thus be needed in order to probe for a deviation from metallic behavior, if any.

For protons, the estimated onset of nonmetallic stopping characteristics lies in the range of about 2.1–4.1 keV where we have taken into account the uncertainty of ~1 eV in the MCSCF calculations for proton projectiles due to restrictions in the active space (reduced number of AUX orbitals). First experiments measuring the stopping power of protons pen-

etrating through LiF foils down to about 2 keV kinetic energy did not show a clear deviation from a linear v_p dependence.[2,5,14] Only in a recent stopping-power experiment using a backscattering geometry[1] a deviation from a linear v_p dependence was found for proton energies below about 3.8 keV in good agreement with our estimate. A deviation from metallic behavior was also found for grazing scattering of low-energy protons at an LiF surface[15] where the onset of the deviation at about 3 keV coincides with our predicted values. In the latter case, however, detailed calculations using a surface cluster (as opposed to bulk clusters studied in this work) are necessary for a direct comparison between theory and experiment.

It is interesting to compare the present results with those of Pruneda *et al.*[13] which seem to indicate a stopping-power threshold at about 1 keV for both protons and antiprotons. While our present calculations suggest a higher threshold for p, for $\bar{p}$ the thresholds should be at lower energy than predicted by Pruneda *et al.* It is therefore premature to draw definite predictions from this comparison as these calculations focus on complementary aspects. The TDDFT calculations include dynamical effects absent in our treatment. On the other hand, the present quasistatic calculation accounts for the electronic structure and the band gap on a considerably improved level of accuracy compared to a (TD)DFT calculation on the LDA level. We hope that future experiments at even lower energies will clarify this issue.

V. CONCLUSIONS

We have performed *ab initio* calculations to study the influence of antiprotons ($\bar{p}$) and protons (p) on the electronic structure of LiF using the embedded-cluster method. We apply SCF as well as MCSCF methods. For a proton projectile a moderate reduction in the excitation energy is found. From the corresponding excitation threshold we estimate a deviation from the proportionality $dE/dx \propto v_p$ for kinetic proton energies below 3.1 ± 1 keV in good agreement with experiment.

For antiprotons much more dramatic changes are predicted. The effective excitation gap is drastically suppressed. For specific configurations, when an antiproton is near an F^- ion, it is reduced to well below 1 eV and, within the accuracy of the present calculation, consistent with a vanishing gap. This is to be compared with the band gap of 14 eV of the unperturbed LiF crystal. The obtained excitation gap constitutes an upper bound, so that we estimate the onset of a deviation from metallic behavior in LiF to projectile energies in the range of several tens of eV. Consequently, in order to reveal such a deviation in future stopping-power experiments with antiprotons, projectile energies down to the eV range should be used. Of course, at such low energies nuclear stopping becomes increasingly important, so that the experimental study of electronic stopping is complicated by this energy-loss channel. With the advent of intense sources of slow antiprotons at FLAIR/FAIR (GSI, Darmstadt) in the not so distant future these predictions could be put to a rigorous test.

ACKNOWLEDGMENTS

This work was supported by the FWF Austria under Project No. P17449-N02, by the ÖAD under Project No. FR 02/2007, by the PHC Amadeus of the French Ministry of Foreign and European Affairs, and by EU network ITSLEIF under Contract No. RII3#026015. We thank H. Lischka and M. Ruckenbauer for their helpful assistance with COLUMBUS.

[1] M. Draxler, S. P. Chenakin, S. N. Markin, and P. Bauer, Phys. Rev. Lett. **95**, 113201 (2005).
[2] S. P. Møller, A. Csete, T. Ichioka, H. Knudsen, U. I. Uggerhøj, and H. H. Andersen, Phys. Rev. Lett. **93**, 042502 (2004).
[3] S. P. Møller, A. Csete, T. Ichioka, H. Knudsen, U. I. Uggerhøj, and H. H. Andersen, Phys. Rev. Lett. **88**, 193201 (2002).
[4] M. Peñalba, J. I. Juaristi, E. Zarate, A. Arnau, and P. Bauer, Phys. Rev. A **64**, 012902 (2001).
[5] J. I. Juaristi, C. Auth, H. Winter, A. Arnau, K. Eder, D. Semrad, F. Aumayr, P. Bauer, and P. M. Echenique, Phys. Rev. Lett. **84**, 2124 (2000).
[6] S. P. Møller, E. Uggerhøj, H. Bluhme, H. Knudsen, U. Mikkelsen, K. Paludan, and E. Morenzoni, Phys. Rev. A **56**, 2930 (1997).
[7] J. C. Ashley, R. H. Ritchie, and W. Brandt, Phys. Rev. B **5**, 2393 (1972).
[8] J. D. Jackson and R. L. McCarthy, Phys. Rev. B **6**, 4131 (1972).
[9] H. Bichsel, Phys. Rev. A **41**, 3642 (1990).
[10] E. V. Alonso, R. A. Baragiola, J. Ferrón, M. M. Jakas, and A. Oliva-Florio, Phys. Rev. B **22**, 80 (1980).
[11] P. Roncin, J. Villette, J. P. Atanas, and H. Khemliche, Phys. Rev. Lett. **83**, 864 (1999).
[12] N.-P. Wang, M. Rohlfing, P. Krüger, and J. Pollmann, Phys. Rev. B **67**, 115111 (2003).
[13] J. M. Pruneda, D. Sánchez-Portal, A. Arnau, J. I. Juaristi, and E. Artacho, Phys. Rev. Lett. **99**, 235501 (2007).
[14] K. Eder, D. Semrad, P. Bauer, R. Golser, P. Maier-Komor, F. Aumayr, M. Peñalba, A. Arnau, J. M. Ugalde, and P. M. Echenique, Phys. Rev. Lett. **79**, 4112 (1997).
[15] C. Auth, A. Mertens, H. Winter, and A. Borisov, Phys. Rev. Lett. **81**, 4831 (1998).
[16] P. A. Zeijlmans van Emmichoven, A. Niehaus, P. Stracke, F. Wiegershaus, S. Krischok, V. Kempter, A. Arnau, F. J. Garcia de Abajo, and M. Peñalba, Phys. Rev. B **59**, 10950 (1999).
[17] U. Fano and W. Lichten, Phys. Rev. Lett. **14**, 627 (1965).
[18] E. Fermi and E. Teller, Phys. Rev. **72**, 399 (1947).
[19] P. V. Sushko, A. L. Shluger, and C. R. A. Catlow, Surf. Sci. **450**, 153 (2000).
[20] L. Wirtz, J. Burgdörfer, M. Dallos, T. Müller, and H. Lischka, Phys. Rev. A **68**, 032902 (2003).
[21] B. Solleder, L. Wirtz, and J. Burgdörfer, Phys. Rev. B **78**, 155432 (2008).
[22] L. D. Landau, Phys. Z. Sowjetunion **2**, 46 (1932); C. Zener, Proc. R. Soc. London, Ser. A **137**, 696 (1932); E. C. G. Stück-

elberg, Helv. Phys. Acta **5**, 361 (1932).
[23] W. Rosen and C. Zener, Phys. Rev. **40**, 502 (1932).
[24] R. Shepard, *The Multiconfiguration Self-Consistent Field Method*, Advances in Chemical Physics: *Ab Initio* Methods in Quantum Chemistry II Vol. 69 (Wiley, New York, 1987), pp. 63–200.
[25] H. Lischka R. Shepard, R. M. Pitzer, I. Shavitt, M. Dallos, Th. Müller, P. G. Szalay, M. Seth, G. S. Kedziora, S. Yabushita, and Z. Zhang, Phys. Chem. Chem. Phys. **3**, 664 (2001); H. Lischka *et al.*, Computer code COLUMBUS, an ab initio electronic structure program, release 5.9.1 2006.
[26] A. Schäfer, H. Horn, and R. Ahlrichs, J. Chem. Phys. **97**, 2571 (1992); A. Schäfer, C. Huber, and R. Ahlrichs, *ibid.* **100**, 5829 (1994).
[27] The quantum-chemistry notation $(7s,3p)/[3s2p]$ reads as follows: this basis set consists of three *s*-type and two *p*-type (contracted) functions which are built up by linear combinations of seven *s*-type and three *p*-type (primitive) Gauss functions, respectively.
[28] T. Veszprémi and M. Fehér, *Quantum Chemistry: Fundamentals to Applications* (Kluwer, New York/Plenum, New York, 1999).
[29] A. B. Kunz, Phys. Rev. B **26**, 2056 (1982).
[30] F. J. Himpsel, L. J. Terminello, D. A. Lapiano-Smith, E. A. Eklund, and J. J. Barton, Phys. Rev. Lett. **68**, 3611 (1992).